INFORMATION TECHNOLOGIES AND AUTOMATIC CONTROL IN FERROUS METALLURGY / **ИНФОРМАЦИОННЫЕ ТЕХНОЛОГИИ И АВТОМАТИЗАЦИЯ В ЧЕРНОЙ МЕТАЛЛУРГИИ**

UDC 669.18
DOI 10.17073/0368-0797-2026-1-84-90

Original article
Оригинальная статья

Modeling of shrinkage processes in slabs during steel casting in continuous casting machines

A. A. Chuev ✉, **S. V. Lukin**

Cherepovets State University (5 Lunacharskogo Ave., Cherepovets, Vologda Region 162600, Russian Federation)

✉ aachuev@chsu.ru

Abstract. Mathematical model of the shrinkage process in a continuously cast slab during its cooling and solidification is proposed. The model is based on solution of the equation of non-stationary thermal conductivity and provisions of the theory of a quasi-equilibrium two-phase zone. Unlike previously proposed models of the slab cooling and solidification process, the proposed one takes into account the dependence of thermal properties of the steel on temperature, as well as such features as chemical composition of the cast steel, geometric shape of the slab cross-section and the process parameters of casting rate and intensity of slab cooling in the secondary cooling zone. The model implements the solution of the heat conductivity equation using the finite difference method, approximation of partial derivatives is performed according to an explicit scheme. During modeling, the temperature field is calculated in the computational domain, which is a quarter of the slab cross-section. In this case, the boundary conditions in the mold and cooling sections of the secondary cooling zone of continuous casting machine are taken into account. The model also implements calculation of the total shrinkage in the slab from the moment of crystallization and also can be used to calculate the shrinkage cavity depth formed in the slab after casting. The model adequacy is confirmed by verification performed by comparing the modeling data with experimental data on the shrinkage cavity depth. Dependence of the modeling accuracy on the number of computational grid nodes is also revealed. The presented model allows calculating the shrinkage cavity depth and developing recommendations for adjusting the mold taper and the parameters of continuous casting machine roller guide depending on the amount of metal shrinkage during cooling and solidification of continuously cast slabs.

Keywords: continuous casting, shrinkage, slab, mathematical model, shrinkage cavity, crystallization, two-phase zone, heat capacity, numerical methods

For citation: Chuev A.A., Lukin S.V. Modeling of shrinkage processes in slabs during steel casting in continuous casting machines. *Izvestiya. Ferrous Metallurgy*. 2026;69(1):84–90. https://doi.org/10.17073/0368-0797-2026-1-84-90

Моделирование процессов усадки в слябах при разливке стали в машинах непрерывного литья заготовок

А. А. Чуев ✉, **С. В. Лукин**

Череповецкий государственный университет (Россия, 162600, Вологодская обл., Череповец, пр. Луначарского, 5)

✉ aachuev@chsu.ru

Аннотация. Предложена математическая модель усадочного процесса в непрерывнолитом слябе при его охлаждении и затвердевании. В основе модели лежат решение уравнения нестационарной теплопроводности и положения теории о квазиравновесной двухфазной зоне. В отличие от ранее предложенных моделей процесса охлаждения и затвердевания сляба, предлагаемая модель учитывает зависимость теплофизических свойств стали от температуры, а также такие особенности, как химический состав разливаемой стали, геометрическую форму поперечного сечения сляба и технологические параметры скорости разливки и интенсивности охлаждения сляба в зоне вторичного охлаждения. Модель реализует решение уравнения теплопроводности с помощью метода конечных разностей, аппроксимация частных производных выполнена по явной схеме. В ходе моделирования производится вычисление температурного поля в расчетной области, представляющей собой четверть поперечного сечения сляба. При этом учитываются граничные условия в кристаллизаторе и секциях охлаждения зоны вторичного охлаждения машины непрерывного литья заготовок. Также модель реализует расчет суммарной усадки в слябе с момента начала кристаллизации. С помощью модели возможно вычисление глубины усадочной раковины, образующейся в слябе после разливки. Адекватность модели подтверждена верификацией, выполненной путем сравнения данных моделирования с экспериментальными данными по глубине усадочной раковины. Выявлена зависимость точности моделирования от количества узлов расчетной сетки. Представленная модель позволяет рассчитывать глубину усадочной раковины и разрабатывать рекомендации по настройке конусности кристаллизатора и параметров роликовой проводки машины непрерывного литья заготовок в зависимости от величины усадки металла при охлаждении и затвердевании непрерывнолитых слябов.

Ключевые слова: непрерывная разливка, усадка, сляб, математическая модель, усадочная раковина, кристаллизация, двухфазная зона, теплоемкость, численные методы

Для цитирования: Чуев А.А., Лукин С.В. Моделирование процессов усадки в слябах при разливке стали в машинах непрерывного литья заготовок. *Известия вузов. Черная металлургия*. 2026;69(1):84–90. https://doi.org/10.17073/0368-0797-2026-1-84-90

Introduction

One of the most important technological processes in modern metallurgy is continuous casting. During the cooling and solidification of a slab in a continuous casting machine (CCM), metal shrinkage occurs, resulting in the formation of a shrinkage cavity in the upper part of the final slab. Of particular interest is the development of a method for calculating the shrinkage of a continuously cast slab in the mold and the secondary cooling zone (SCZ) of a CCM, as well as determining the slab dimensions with shrinkage taken into account. A number of mathematical models describing the processes of slab cooling and metal shrinkage have been developed. Research on this topic began in the 1970s. For example, study [1] was devoted to calculating shrinkage during solidification of a billet with a circular cross-section. Subsequently, the developed models became more sophisticated, incorporating hydrodynamic phenomena in the liquid phase [2], more detailed descriptions of slab bulging [3], phase transformations during casting [4], thermomechanical phenomena [5], heat transfer in the secondary cooling zone [6], and other factors.

The development of a predictive shrinkage model would make it possible to account for the influence of shrinkage on technological parameters such as mold taper and the roller gap in the SCZ. In study [7], an attempt was made to predict the "ideal" mold taper using a two-dimensional mathematical model. Attempts were also made to develop a model that takes into account the carbon content in steel [8].

In Russian research, particular attention has been given to the works of Dyudkin D.A. [9] and Samoylovich Yu.A. and Kabakov Z.K. [10; 11], who developed a universal model describing the cooling and solidification of a continuously cast slab. This model subsequently formed the basis for numerous further developments, including models of slab surface layer formation [12], continuous slab deformation [13], and the secondary cooling zone (SCZ) system of the CCM [14; 15], among others.

Most proposed models assume that the thermal properties of the metal are independent of temperature. In many cases, these properties are taken as constant for both the solid and liquid phases. When reliable temperature-dependent data are unavailable, the properties are typically estimated by linear interpolation. Moreover, the calculated shrinkage parameters strongly depend on the selected numerical method: study [16] shows that results obtained using different models for identical input data may differ by more than a factor of two.

Thus, the existing models of shrinkage processes are not universal and remain imperfect, since they do not account for all features of slab solidification and cooling in a CCM. Therefore, there is a need to develop a more comprehensive mathematical model of shrinkage processes in continuously cast slabs.

Fundamental theoretical provisions

The mathematical model of cooling and solidification of a continuously cast slab is based on the solution of the transient heat conduction equation:

$$c_{\text{eff}}\,\rho\left(\frac{\partial T}{\partial t}+v\frac{\partial T}{\partial z}\right)=\frac{\partial}{\partial x}\left(\lambda\frac{\partial T}{\partial x}\right)+\frac{\partial}{\partial z}\left(\lambda\frac{\partial T}{\partial z}\right)+\Theta(x,y,t),$$
$$0\le t\le t_{\text{c}},\ 0\le x\le B,\ 0\le z\le h, \qquad (1)$$

where c_{eff} is the effective heat capacity of steel; ρ is the steel density; λ is the thermal conductivity of the melt; B is half of the slab thickness, m; h is the slab height, m; v is the slab withdrawal rate along the vertical axis, m/min; Θ is the heat source of superheated metal in the region influenced by the casting jet.

$$c_{\text{eff}}=\begin{cases}c_{\text{m}},\ T<T_{\text{s}},\ T>T_{\text{l}};\\ c_{\text{m}}-L\dfrac{d\psi}{dT},\ T_{\text{s}}\le T\le T_{\text{l}},\end{cases} \qquad (2)$$

where c_{m} is the molecular heat capacity of the alloy; T_{s} and T_{l} are the solidus and liquidus temperatures, respectively; L is the latent heat of solidification of the metal in the solid–liquid (two-phase) zone; $\dfrac{d\psi}{dT}$ is the rate of phase transformation during equilibrium solidification of the binary alloy.

Since metal solidification depends on the percentage carbon content, establishing the temperature dependence $c_{\text{eff}}(T)$ requires consideration of the Fe–C phase diagram, particularly its high-temperature part (Fig. 1).

The diagram shown in Fig. 1 identifies three steel groups: *I* – [% C] ≤ 0.1; *II* – 0.1 < [% C] ≤ 0.16; *III* – 0.16 < [% C] ≤ 0.5. For each group, the temperature dependence $c_{\text{eff}}(T)$ was determined, where:

$$c_I(T)=c_M-\begin{cases}0,\ T<T_{NJ};\ T_{NH}\le T<T_{AH};\ T\ge T_{AB},\\ L_{1-\delta}\dfrac{d\psi_\delta}{dT},\ T_{AH}\le T<T_{AB};\\ L_{\delta-\gamma}\dfrac{d\psi_\gamma}{dT},\ T_{NJ}\le T<T_{NH},\end{cases} \qquad (3)$$

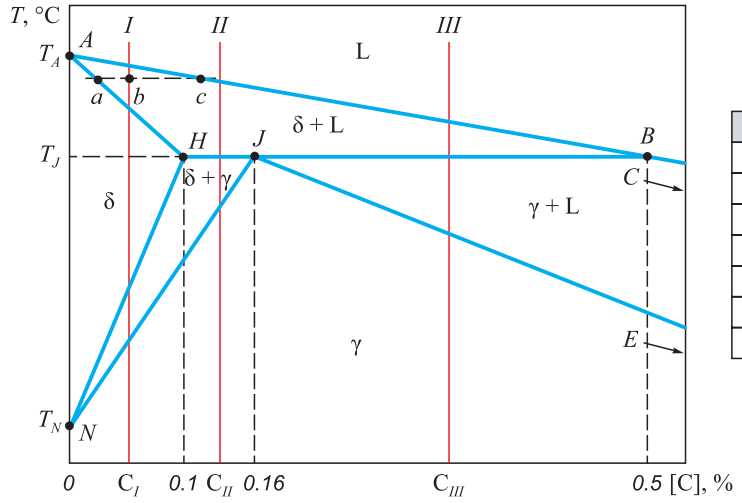

Point	*T*, °C	[C], %
A	1539	0
B	1499	0.50
C	1147	4.30
E	1147	2.14
J	1499	0.16
H	1499	0.10
N	1392	0

Fig. 1. High-temperature part of Fe–C diagram

Рис. 1. Высокотемпературная область диаграммы Fe–C

where $L_{1-\delta}$ is the latent heat of the liquid → δ-ferrite transformation; $L_{\delta-\gamma}$ is the latent heat of the δ-ferrite → austenite transformation; ψ_δ is the volume fraction of δ-ferrite in the elementary volume of the "liquid + δ-ferrite" mixture; ψ_γ is the volume fraction of austenite in the "δ-ferrite + austenite" mixture; $\frac{d\psi_\delta}{dT}$ and $\frac{d\psi_\gamma}{dT}$ are the rates of formation of δ-ferrite and austenite, respectively.

$$c_{II}(T) = c_M + \delta(T - T_J)Q_1 - \begin{cases} 0, \ T < T_{NJ}; \ T \geq T_{AB}, \\ L_{1-\delta}\dfrac{d\psi_\delta}{dT}, \ T_J \leq T < T_{AB}; \\ L_{\delta-\gamma}\dfrac{d\psi_\gamma}{dT}, \ T_{NJ} \leq T < T_J, \end{cases} \quad (4)$$

where $\delta(T)$ is the Dirac delta function, which was approximated by the expression $\delta(x) \approx \frac{1}{a\sqrt{\pi}} e^{-\left(\frac{x}{a}\right)^2}$;

$$c_{III}(T) = c_M + \delta(T - T_J)Q_2 - \begin{cases} 0, \ T < T_{JE}; \ T \geq T_{AB}, \\ L_{1-\delta}\dfrac{d\psi_\delta}{dT}, \ T_J \leq T < T_{AB}; \\ L_{1-\gamma}\dfrac{d\psi_\gamma}{dT}, \ T_{JE} \leq T < T_J. \end{cases} \quad (5)$$

Similarly, the temperature dependences of the effective thermal conductivity $\lambda_{eff}(T)$ and the density $\rho(T)$ were determined.

The calculation of the linear shrinkage coefficient $\alpha_l(T)$ was carried out based on the obtained values of the thermal parameters. Since the temperature dependence of the specific volume $V(T)$ in the Fe–C system is strongly influenced by the carbon concentration, it can be concluded that a similar dependence also applies to linear shrinkage. In the proposed model, the coefficient $\alpha_l(T)$ is calculated using the expression for volumetric shrinkage given in [17]:

$$\alpha_V(T) = \frac{dV(T)}{dT}\frac{1}{V(T)}, \quad (6)$$

where $V(T)$ is the temperature-dependent specific volume of the alloy; $\frac{dV(T)}{dT}$ is the temperature derivative of the specific volume.

The calculated values of the volumetric shrinkage coefficient $\alpha_V(T)$ are subsequently used to determine the shrinkage cavity depth [18].

To solve equation (1), the finite difference method (FDM) was applied using an explicit scheme for approximating the partial derivatives, with the introduction of fictitious nodes that allow more accurate approximation of boundary derivatives with respect to *x* and *y*. The computational domain represents one quarter of the slab cross-section (Fig. 2). The number of nodes in the region $0 \leq x \leq A$ is taken as *N*, and in the region $0 \leq x \leq B$ as *M*.

At the initial time, the temperature is assumed to be uniform and equal to the liquidus temperature:

$$T(0, x, y) = T_l = \text{const}. \quad (7)$$

The boundary conditions on boundaries Γ_3 and Γ_4 are:

$$\lambda\frac{\partial T}{\partial w} = 0, \text{ where } w = x, y. \quad (8)$$

The boundary conditions for the cooling zones along boundary Γ_1 are defined as follows:

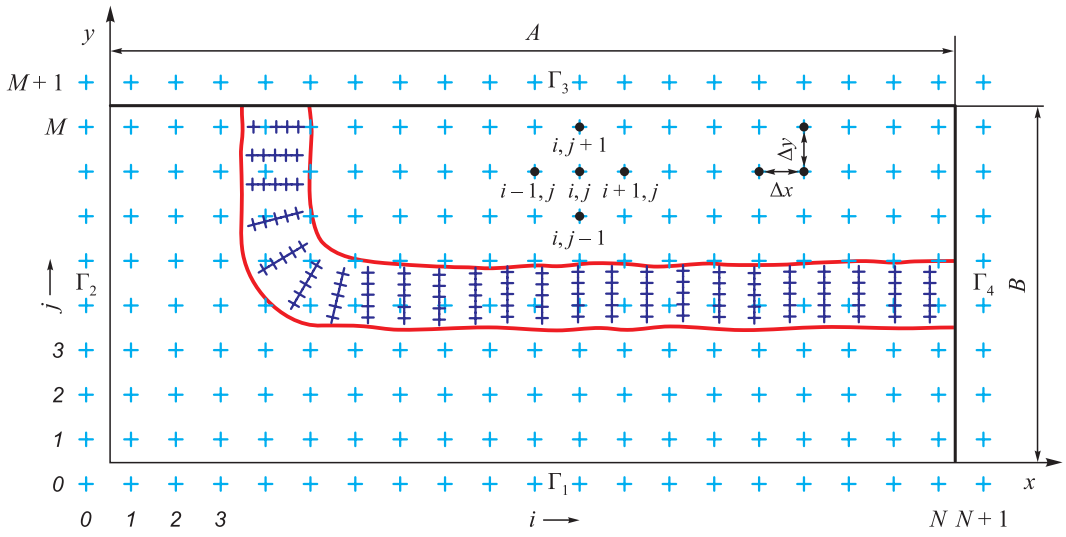

Fig. 2. Scheme of discretization of the computational domain. Nodes 0, $N + 1$, $M + 1$ – fictitious, the rest – internal

Рис. 2. Схема дискретизации расчетной области. Узлы 0, $N + 1$, $M + 1$ – фиктивные, остальные внутренние

– in the mold:

$$q = \alpha_m(T_s - T_w), \quad (9)$$

where α_m is the heat transfer coefficient in the mold; $q = -\lambda\frac{\partial T}{\partial w}$, where $w = x, y$ is the heat flux from one face of the slab;

– in the i-th SCZ section:

$$\lambda\frac{\partial T}{\partial w} = \alpha_i(T_s - T_{am}), \text{ where } w = x, y; \quad (10)$$

– air cooling:

$$\lambda\frac{\partial T}{\partial w} = \alpha_1\left(T_s - T_{am}\right),$$
$$\alpha_1 = \sigma_1\left(T_s^2 + T_{am}^2\right)\left(T_s + T_{am}\right) + \alpha_c, \quad (11)$$

where α_i is the heat transfer coefficient in the i-th SCZ section; T_s is the slab surface temperature; T_w is the temperature of the cooling water in the mold; T_m is the temperature of the working (copper) wall of the mold; T_{am} is the ambient temperature; σ_1 is the radiation coefficient; α_1 is the effective heat transfer coefficient during air cooling; α_c is the convective heat transfer coefficient Boundary conditions on Γ_2 are specified in a similar manner.

The procedure for calculating linear shrinkage is as follows. The calculation is performed for one quarter of the slab cross-section, and the solidus isotherm is taken as the boundary of complete solidification. In [19], an expression was obtained for the relative strain rate of the solid shell:

$$\eta = \frac{1}{\xi}\int_0^{\xi}\alpha_l(T)\dot{T}dx, \quad (12)$$

where ξ is the thickness of the solid shell; $\alpha_l(T)$ is the linear shrinkage coefficient of steel; $\dot{T}$ is the temperature change rate at point x at time t.

After integrating this expression over the width of the face, the strain rate expressions for the wide face (η_{wf}) and narrow face (η_{nf}) of the slab are obtained. The total deformation of the faces from the onset of solidification is then determined:

$$\eta_{\Sigma_{wf}} = \int_0^t\frac{1}{\xi_{wf}}\int_0^{A(t)}\int_0^{\xi_{wf}}\alpha_l(T)\dot{T}dydxdt; \quad (13)$$

$$\eta_{\Sigma_{nf}} = \int_0^t\frac{1}{\xi_{nf}}\int_0^{B(t)}\int_0^{\xi_{nf}}\alpha_l(T)\dot{T}dxdydt, \quad (14)$$

where ξ_{wf} and ξ_{nf} are the thicknesses of the solidified layer at the wide and narrow faces, respectively, mm; $\alpha_l(T)$ is the linear shrinkage coefficient, °C^{-1}; $\dot{T}$ is the rate of temperature decrease/increase at point x at time t, °C/s.

Then, the slab thickness and width during solidification are determined as follows

$$x_A^{n+1} = 2A\left(1 - \eta_{\Sigma_{wf}}^{n+1}\right); \quad (15)$$

$$x_B^{n+1} = 2B\left(1 - \eta_{\Sigma_{nf}}^{n+1}\right). \quad (16)$$

Verification

The model was implemented as a computer program. The following input data were used in the simu-

Table 1. **Size of crystallizer and sections of secondary cooling zone**

Таблица 1. **Размер кристаллизатора и секций ЗВО**

Section	Mold	SCZ section number								
		1	*2*	*3*	*4*	*5*	*6*	*7*	*8*	*9*
l, m	0.8	0.200	1.200	1.980	1.620	1.660	1.834	1.816	3.450	5.170
α_i, W/(m^2·K)	456	620	428	281	281	0	0	0	0	0

lations: slab thickness B = 0.2 m, slab height h = 6.5 m, initial temperature T_0 = 1520 °C, ambient temperature T_{am} = 30 °C, liquidus temperature T_l = 1500 °C, solidus temperature T_s = 1450 °C, number of nodes across the thickness M = 20, number of nodes across the height N = 2500, casting rate v = 0.4 m/min, and cross-section 200×1200 mm. The mold length, SCZ section lengths, and the heat transfer coefficients for the individual sections are given in Table 1.

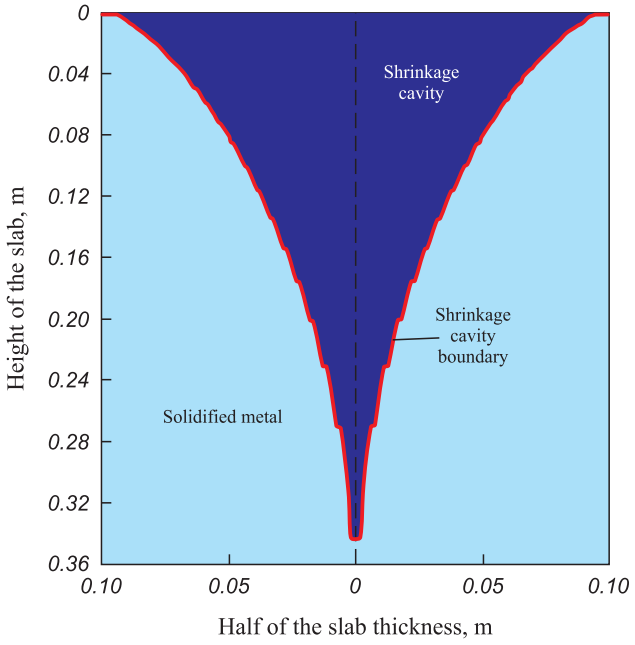

Fig. 3. Calculated shrinkage cavity profile

Рис. 3. Рассчитанный профиль усадочной раковины

Verification was performed by comparing the calculated shrinkage cavity depth with the experimental data reported in [20]. According to [20], the mean cavity depth for a sample of 26 slabs is 0.353 m. In turn, the shrinkage cavity depth obtained in the simulation was 0.35 m (Fig. 3).

During verification, the dependence of the relative modeling error on the number of grid nodes along the height N and thickness M was also identified (see Tables 2 and 3).

Tables 2 and 3 show that modeling accuracy increases with increasing numbers of nodes along the height and thickness, reaching an acceptable level of <5 % at N = 2500 and M = 20.

CONCLUSIONS

A mathematical model of the shrinkage process in a continuously cast slab has been developed. Its distinctive feature is the incorporation of temperature-dependent thermal properties of the metal and technological casting parameters.

Table 2. **Dependence of shrinkage cavity depth on the number of nodes by height**

Таблица 2. **Зависимость глубины усадочной раковины (УР) от числа узлов по высоте**

Number of nodes along the height, N	2500	2000	1500	1000	500	200
Shrinkage cavity depth, m (calculated)	0.35	0.33	0.32	0.31	0.31	0.30
Shrinkage cavity depth, m (experimental)	0.353	0.353	0.353	0.353	0.353	0.353
Relative error, %	0.85	6.52	9.35	12.18	12.18	15.01

Table 3. **Dependence of shrinkage cavity depth on the number of nodes by thickness**

Таблица 3. **Зависимость глубины усадочной раковины от числа узлов по толщине**

Number of nodes across the thickness, M	20	19	18	17
Shrinkage cavity depth, m (calculated)	0.35	0.35	0.37	0.41
Shrinkage cavity depth, m (experimental)	0.353	0.353	0.353	0.353
Relative error, %	0.85	0.85	4.82	16.15

Model verification confirmed the agreement between the simulation results, theoretical calculations, and experimental data.

The modeling accuracy increases with increasing numbers of computational grid nodes along the height N and thickness M, with M having a stronger effect on the modeling accuracy.

The proposed model can be used to improve continuous casting technology.

References / Список литературы

1. Bauman H.G., Schafer G. Beitrag zur Berechnung der Kontraktion von Stahl Während seiner Erstarrung. *Archiv für das Eisenhüttenwesen*. 1970;41(12):1111–1115. (In Germ.).
2. Telejko T., Malinowsky Z., Rywotycki M. Analysis of heat transfer and fluid flow in continuous steel casting. *Archives of Metallurgy and Materials*. 2009;54(3):837–844.
3. Wu D., Li J., Qin Q., Ma T. Research on creep material models and bulging of cast slab. In: *2010 Int. Conf. on Mechanic Automation and Control Engineering, Wuhan, China*; 2010:5536–5539. https://doi.org/10.1109/MACE.2010.5535615
4. Chimani C.M., Resch H., Mörwald K., Kolednik O. Precipitation and phase transformation modelling to predict surface cracks and slab quality. *Ironmaking & Steelmaking*. 2005;32(1):75–79. https://doi.org/10.1179/174328105X15814
5. Zappulla M.L.S., Thomas B.G., Hibbeler L.C. Effect of grade on thermal-mechanical behavior of steel during initial solidification. *Metallurgical and Materials Transactions A*. 2017;48(8):1–17. https://doi.org/10.1007/s11661-017-4112-z
6. Assuncao C., Tavares R., Oliveira G. Improvement in secondary cooling of continuous casting of round billets through analysis of heat flux distribution. *Ironmaking & Steelmaking*. 2015;42(1):1–8. https://doi.org/10.1179/1743281214Y.0000000190
7. Li C., Thomas B.G., Storkman W.R., Moitra A. Ideal mold taper prediction using CON2D. In: *Proceedings of the 9th Int. Iron and Steel Congress, Nagoya, Japan, Iron & Steel Inst. Japan, Tokyo*.1999;3:348–355.
8. Zhu L.-G., Kumar R.V. Shrinkage of carbon steel by thermal contraction and phase transformation during solidification. *Ironmaking & Steelmaking*. 2007;34(1):71–75. https://doi.org/10.1179/174328106X118143
9. Dyudkin D.A., Krupman L.I., Maksimenko D.M. Shrinkage Cavities in Steel Ingots and Billets. Moscow: Metallurgiya; 1983:137. (In Russ.).

   Дюдкин Д.А., Крупман Л.И., Максименко Д.М. Усадочные раковины в стальных слитках и заготовках. Москва: Металлургия; 1983:137.
10. Samoilovich Yu.A., Kabakov Z.K. Taking into account the effect of stress relaxation when determining thermal stresses in a casting. In: *Combustion, Heat Transfer and Heating of Metal: Proceedings*. Moscow: Metallurgiya; 1973;(24): 100–113. (In Russ.).

    Самойлович Ю.А., Кабаков З.К. Учет эффекта релаксации напряжений при определении термических напряжений в отливке. *Горение, теплообмен и нагрев металла: Сборник научных трудов*. Москва: Металлургия; 1973;(24):100–113.
11. Samoilovich Yu.A., Kabakov Z.K., Goryainov V.A., Perminov V.P., Podorvanov A.G., Sakhnov B.I. Application of mathematical models to study the processes of solidification and cooling of continuous steel ingots of rectangular cross-section. In: *Nepreryvnaya Razlivka Stali*. Moscow: Metallurgiya; 1974;(2):44–49. (In Russ.).

    Самойлович Ю.А., Кабаков З.К., Горяинов В.А., Перминов В.П., Подорванов А.Г., Сахнов Б.И. Применение математических моделей для исследования процессов затвердевания и охлаждения непрерывных стальных слитков прямоугольного поперечного сечения. *Непрерывная разливка стали*. Москва: Металлургия; 1974;(2):44–49.
12. Khasin G.A. On mathematical modeling of formation of ingot surface layers. *Izvestiya. Ferrous Metallurgy*. 1987;30(8):133–135. (In Russ.).

    Хасин Г.А. О математическом моделировании процесса формирования поверхностных слоев слитка. *Известия вузов. Черная металлургия*. 1987;30(8):133–135.
13. Danilov V.L., Korablin A.I. Mathematical model of deformation of continuously cast steel slabs. *BMSTU Journal of Mechanical Engineering*. 1989;(12):142–145. (In Russ.).

    Данилов В.Л., Кораблин А.И. Математическая модель деформирования непрерывнолитых стальных слябов. *Известия вузов. Машиностроение*. 1989;(12):142–145.
14. Yaukhola M., Kivelya E., Konttinen Yu., Laitinen E. Dynamic model of the secondary cooling zone cooling system for continuous casting machines. *Stal'*. 1995;(2):25–29. (In Russ.).

    Яухола М., Кивеля Э., Конттинен Ю., Лайтинен Э. Динамическая модель системы охлаждения вторичной зоны охлаждения для машин непрерывного литья заготовок. *Сталь*. 1995;(2):25–29.
15. Devyatov D.Kh., Panteleev I.I. Determination of heat transfer coefficients in CCM secondary cooling zone using identifiable mathematical model. *Izvestiya. Ferrous Metallurgy*. 1999;42(8):62–65. (In Russ.).

    Девятов Д.Х., Пантелеев И.И. Определение коэффициентов теплоотдачи в зоне вторичного охлаждения МНЛЗ с помощью идентифицируемой математической модели. *Известия вузов. Черная металлургия*. 1999;42(8):62–65.
16. Meng Y., Li C., Parkman J., Thomas B.G. Simulation of shrinkage and stress in solidifying steel shells of different grade. In: *Solidification Processes and Microstructures: A Symposium in Honor of Wilfried Kurz edited by M. Rappaz TMS (The Minerals, Metals & Materials Society), Charlotte, NC*. 2004:33–39.
17. Thomas B.G., Ojeda C. Ideal taper prediction for slab casting. In: *2003 ISSTech Steelmaking Conf., Indianapolis, IN, USA, April 27-30, 2003, ISS-AIME, Warrendale, PA*. 2003:295–308.
18. Kabakov Z.K., Gabelaya D.I., Chuev A.A. Mathematical model of formation of shrinkage cavity of continuously cast billet on continuous casting machine. In: *13th Int. Sci. and Tech. Conf. "INFOS-2022": Proceedings*. Vologda: VSU; 2022:14–18. (In Russ.).

    Кабаков З.К., Габелая Д.И., Чуев А.А. Математическая модель формирования усадочной раковины непрерывнолитой заготовки на МНЛЗ. *Тринадцатая Международная научно-техническая конференция «ИНФОС-2022»:*

Труды. Вологда: Вологодский государственный университет; 2022:14–18.

19. Samoilovich Yu.A., Goryainov V.A., Krulevetskii S.A., Kabakov Z.K. Thermal Processes in Continuous Steel Casting. Moscow: Metallurgiya; 1982:152. (In Russ.).

Самойлович Ю.А., Горяинов В.А., Крулевецкий С.А., Кабаков З.К. Тепловые процессы при непрерывном литье стали. Москва: Металлургия; 1982:152.

20. Dyudkin D.A. Conditions for forming the end portion of a continuous ingot. In: *Proceedings of the III Conf. on the Ingot "Problems of the Steel Ingot"*. Moscow: Metallurgiya; 1969:375–381. (In Russ.).

Дюдкин Д.А. Условия формирования концевой части непрерывного слитка. *Материалы III конференции по слитку «Проблемы стального слитка»: Труды*. Москва: Металлургия; 1969:375–381.

Information about the Authors

Anton A. Chuev, *Senior Lecturer of the Chair of Mathematics and Informatics*, Cherepovets State University
ORCID: 0000-0002-4060-6117
E-mail: aachuev@chsu.ru

Sergei V. Lukin, *Dr. Sci. (Eng.), Prof. of the Chair Thermal Power and Heat Engineering*, Cherepovets State University
E-mail: s.v.luk@yandex.ru

Сведения об авторах

Антон Андреевич Чуев, *старший преподаватель кафедры математики и информатики*, Череповецкий государственный университет
ORCID: 0000-0002-4060-6117
E-mail: aachuev@chsu.ru

Сергей Владимирович Лукин, *д.т.н., профессор кафедры теплоэнергетики и теплотехники*, Череповецкий государственный университет
E-mail: s.v.luk@yandex.ru

Contribution of the Authors

A. A. Chuev – literary analysis, implementation of the algorithm, analysis of the obtained data, formation of conclusions.
S. V. Lukin – scientific guidance, problem statement, conceptualization, editing the text.

Вклад авторов

А. А. Чуев – анализ литературных источников, реализация алгоритма, анализ полученных данных, формирование выводов.
С. В. Лукин – научное руководство, постановка задачи, формирование основной концепции, редактирование текста статьи.

Received 29.04.2025
Revised 10.05.2025
Accepted 20.11.2025

Поступила в редакцию 29.04.2025
После доработки 10.05.2025
Принята к публикации 20.11.2025